Edinburgh Research Explorer

Process design and optimisation for the continuous manufacturing of Nevirapine, an Active Pharmaceutical Ingredient (API) for H.I.V. treatment

1
2
3
4
5
6
7
8
9
10
11
12
13
14
15
16
17
18
19
20
21
22
23
24
25
26
27
28
29
30
31
32
33
34
35
36
37
38
39
40
41
42
43
44
45
46
47
48
49
50
51
52
53
54
55
56
57
58
59
60

PROCESS DESIGN AND OPTIMISATION FOR THE CONTINUOUS MANUFACTURING OF NEVIRAPINE, AN ACTIVE PHARMACEUTICAL INGREDIENT (API) FOR H.I.V. TREATMENT

Samir Diab[a], D. Tyler McQuade[b], B. Frank Gupton[b], Dimitrios I. Gerogiorgis[a*]

[a] Institute for Materials and Processes (IMP), School of Engineering, University of Edinburgh, The Kings Buildings, Edinburgh, EH9 3FB, Scotland, UK

[b] Department of Chemical and Life Sciences Engineering, School of Engineering, Virginia Commonwealth University, Richmond (VA) 23284-3028, USA

Corresponding Author: D.Gerogiorgis@ed.ac.uk

ABSTRACT

Development of efficient and cost-effective manufacturing routes towards HIV active pharmaceutical ingredients (APIs) is essential to ensure their global, affordable access. Continuous pharmaceutical manufacturing (CPM) is a new production paradigm for the pharmaceutical industry, whose potential for enhanced efficiency and economic viability over currently implemented batch protocols offers promise for improving HIV API production. Nevirapine is a widely-prescribed HIV API, whose continuous flow synthesis was recently demonstrated. This paper presents technoeconomic optimisation of nevirapine CPM, including the continuous flow synthesis and a conceptual continuous crystallisation. Arrhenius law parameter estimation from published reaction kinetic data allows explicit modelling of the temperature-dependence of reaction performance and an experimentally validated aqueous API solubility computation method is used to model crystallisation processes. A nonlinear optimisation problem for cost minimisation is formulated for comparative evaluation of different plant designs. Higher reactor temperatures are favoured for CPM total cost minimisation, while lower pH (less neutralising agent) is required to attain the desired plant capacities for cost optimal configurations compared to batch crystallisation designs. Suitable *E*-factors for pharmaceutical manufacturing are attained when higher solvent recoveries are assumed. Implementing CPM designs significantly lowers the nevirapine cost of goods towards reducing the price of societally-important HIV medicines.

1. Introduction

Affordability and accessibility of essential medicines remains a pressing issue for the treatment of diseases prevalent in developing countries. The treatment of the human immunodeficiency virus (HIV) continues to be one of the most prominent global health challenges; the prevalence of the virus has been historically increasing worldwide, with low- and middle-income countries being those most affected (Fig. 1). The development of efficient, cost-effective manufacturing routes towards drugs for HIV treatment is paramount to ensure global, affordable access to such medicines.[1]
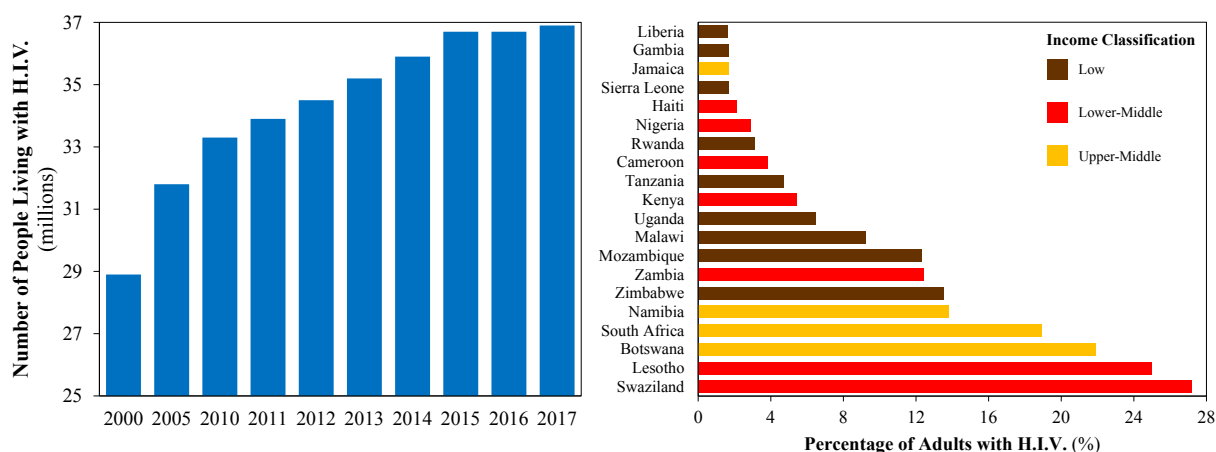

Figure 1: Increasing worldwide HIV prevalence[2] and the top 20 countries with the highest viral rates.[3]

Continuous pharmaceutical manufacturing (CPM) has emerged as a new production paradigm for its promise of enhanced efficiency and greater economic viability over currently implemented batch protocols.[4,5] The utility of CPM platforms for the development of active pharmaceutical ingredients (APIs) for the treatment of HIV and other societally-important diseases, has been demonstrated in the literature;[6,7] Table 1 lists various HIV APIs whose syntheses have benefited by implementing semi-continuous/continuous flow methods. While experimental demonstration of feasible API continuous synthetic routes is the foundation of any CPM campaign,[7,8] the design of continuous separation processes for integration into upstream CPM is essential to realise the benefits of end-to-end continuous manufacturing for HIV API production.[9]

Table 1: Demonstrated continuous/semi-continuous flow syntheses of HIV APIs.

API	Year	Continuous / Semi-Continuous	Processing Benefits	Ref.
Efavirenz	2013	Semi-continuous	Improved API yield Reduced process time Reduced number of unit operations	33
Darunavir	2015	Continuous	End-to-end continuous process at production scale	34, 35
Lamivudine	2017	Semi-continuous	Improved API yield Reduced process time	36
Nevirapine	2017	Continuous	Improved material efficiency Reduced number of unit operations	10
Dolutegravir	2018	Continuous	Reduced process time	37

Nevirapine is a widely-prescribed API for HIV-1 treatment on the World Health Organisation (WHO) List of Essential Medicines, whose continuous flow synthesis from two advanced starting materials was recently demonstrated with subsequent purification and batch crystallisation for final API separation.[10] Additionally, various routes towards one of the API synthesis starting materials, 2-chloro-3-amino-4-picoline (CAPIC), has also been presented in the literature.[11,12] The economic viability of different process alternatives for the API is yet to be systematically investigated and is essential to

ensure cost optimal designs. Systematic comparison of process alternatives is essential to further aid the development of leaner manufacturing routes towards this societally-important HIV API.[13]

Process modelling and optimisation methodologies can be used to establish optimal design configurations.[13,14] Advanced theoretical methods have been previously implemented towards optimal pharmaceutical unit design[15] and optimisation of pharmaceutical manufacturing processes to elucidate optimal operation, analysis of synthetic pathways[16–18] and life-cycle assessments.[19,20] Modelling and optimisation have also been implemented in the design of separation processes in pharmaceutical manufacturing, such as liquid-liquid extraction (LLE),[21–23] crystallisation[24–30] and chromatographic methods.[31] Identification of cost optimal plantwide designs is essential,[15] particularly end-to-end designs encompassing synthesis and purification/separation. Elucidating cost optimal designs for nevirapine CPM will further aid process development for this societally-important API.[5,32]

This work conducts a systematic comparative evaluation of CPM process alternatives for nevirapine based upon the published synthetic routes via steady-state process modelling and optimisation.[10–12] The continuous process for nevirapine demonstrated in the literature are first presented. A conceptual continuous crystallisation process is considered for comparison to the demonstrated batch crystallisation process. Arrhenius parameter estimation from experimental kinetic data allows flow reactor design for the continuous synthesis of nevirapine. Crystallisation process design utilises an established API solubility model.[38] Costing methodologies for pharmaceutical process alternatives are presented.[5] A constrained nonlinear optimisation problem for total cost minimisation of different design alternatives is then formulated. Optimal total cost components, plant material efficiencies and corresponding operating parameters are presented for different process configurations for comparative evaluation to establish the most promising designs for nevirapine production.

2. Process Modelling, Simulation and Optimisation

2.1 API and Starting Material Synthetic Routes

Various commercial routes towards nevirapine have been demonstrated in the literature with varying complexities and material intensities.[39] The recent demonstration of the continuous flow synthesis of nevirapine uses advanced starting materials, 2-chloro-3-amino-4-picoline (CAPIC) and MeCAN (2-(cyclopropylamino)nicotinate).[10] The syntheses of CAPIC and MeCAN are summarised below (Fig. 2).

Fig. 2a illustrates the published batchwise synthesis of CAPIC. Acetone and malononitrile (**2**) react in toluene (PhMe) in the presence of basic Al_2O_3 at 15-20 °C to form ylidene (**3**), followed by filtration of Al_2O_3 from the reaction mixture. Dimethyl formamide-dimethyl-sulfate (DMF-DMS, **4**) and acetic anhydride (Ac_2O) and triethylamine (TEA) are then added to the filtrate under N_2 to form enamine (**5**). Hydrogen chloride (HCl) gas is then bubbled into the reaction mixture and heated to 50 °C. The mixture is then concentrated by evaporating solvent and water followed by filtration of product 2-chloro-4-methylnicotinonitrile (CYCIC, **6**). Sulfuric acid (H_2SO_4) is then added to the solid CYCIC and reacted at high temperature followed by the addition of water. An aqueous solution of NaOH is added at 40 °C until pH = 11. The resulting suspension is then filtered for product 2-chloro-4-methylnicotinamide (COMAD, **7**). A mixture of COMAD, water and sodium hypobromite (NaOBr) is made at 0 °C. Water is then added and the mixture is heated to 80 °C and stirred. After cooling to 50 °C, PhMe is added to form a biphasic mixture; the organic layer is washed with water and concentrated under vacuum to remove solvent. Hexanes are then added to precipitate CAPIC.

Fig. 2b illustrates the published batchwise synthesis of MeCAN. 2-chloronicotinonitrile (**9**), cyclopropylamine (CPA), TEA, water and isopropyl alcohol (IPA) are added at 140 °C and pressurised to 10 psi to form intermediate **10**. The mixture is stirred and then cooled to 60 °C. Potassium hydroxide (KOH) is then added to the reaction mixture and stirred. Concentrated HCl is added to change pH to 6 and cooled to 10 °C to precipitate 2-(cyclopropylamino)nicotinic acid (2-CAN, **11**), which is then vacuum filtered. 2-CAN is then dissolved in PhMe under N_2, adding thionyl chloride ($SOCl_2$). The reaction mixture is cooled to 0 °C followed by H_2O addition and pH adjusted to 9 with NaOH solution (aq.) and a biphasic mixture forms. The aqueous layer is washed with PhMe and the combined organic layers washed with H_2O and dried with Mg_2SO_4, followed by filtration and concentrated under vacuum to yield MeCAN.
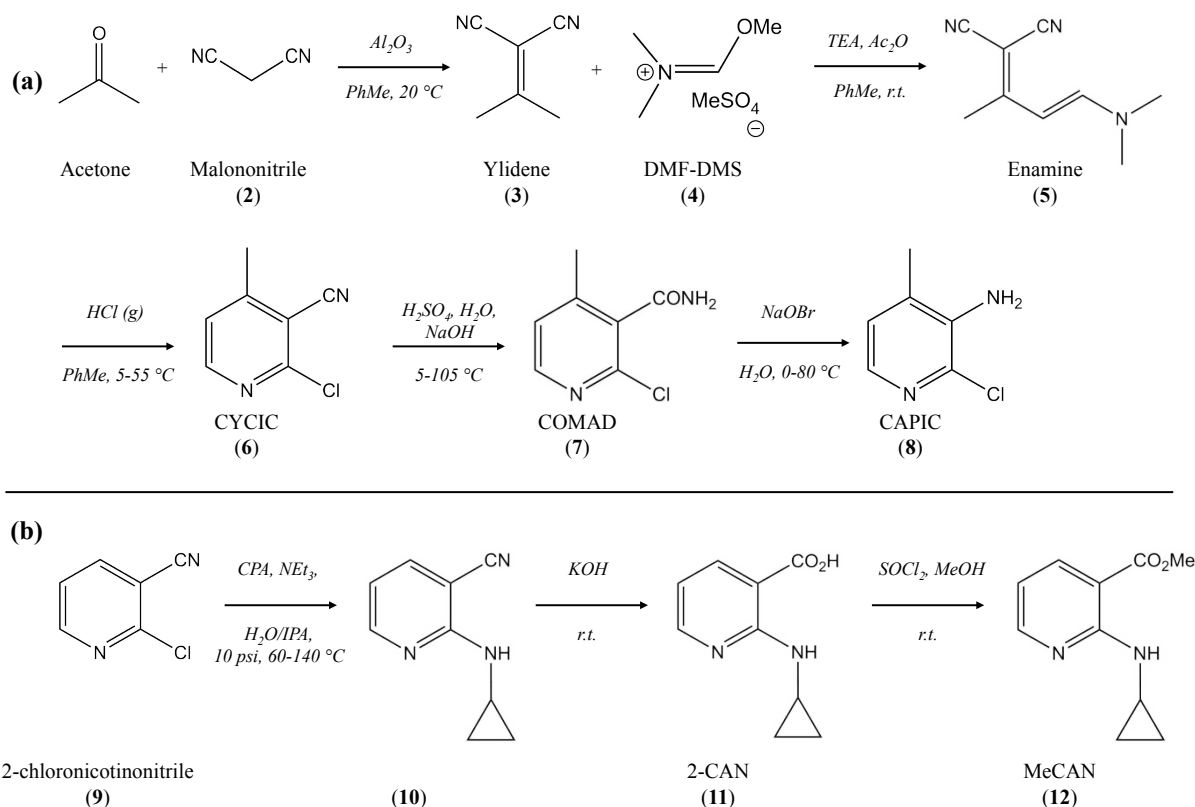
Figure 2: Published batchwise syntheses of (a) CAPIC and (b) MeCAN.[10]

The published continuous synthetic route from CAPIC and MeCAN is shown in Fig. 3.[10] Starting materials CAPIC and MeCAN (in diglyme carrier solvent) are used to form intermediate *N*-(2-chloro-4-methylpyridin-3-yl)-2-(cyclopropylamino)nicotinamide (CYCLOR) in the presence of NaH, which then forms nevirapine (API). The CPM process in this work is based upon this demonstrated continuous flow synthesis; whose process modelling and simulation are further developed in later sub-sections.

Name:	**CAPIC**	**MeCAN**	**CYCLOR**	**API**
	2-chloro-3-amino-4-picoline	methyl 2-(cyclopropyl-amino)nicotinate	*N*-(2-chloro-4-methylpyridin-3-yl)-2-(cyclopropylamino)nicotinamide	Nevirapine
Type:	Reagent	Reagent	Intermediate	Product
Formula:	$C_6H_7ClN_2$	$C_{10}H_{12}N_2O_2$	$C_{10}H_{12}N_2O_2$	$C_{15}H_{14}N_4O$
MW (g mol^{-1}):	142.59	192.21	192.21	266.30

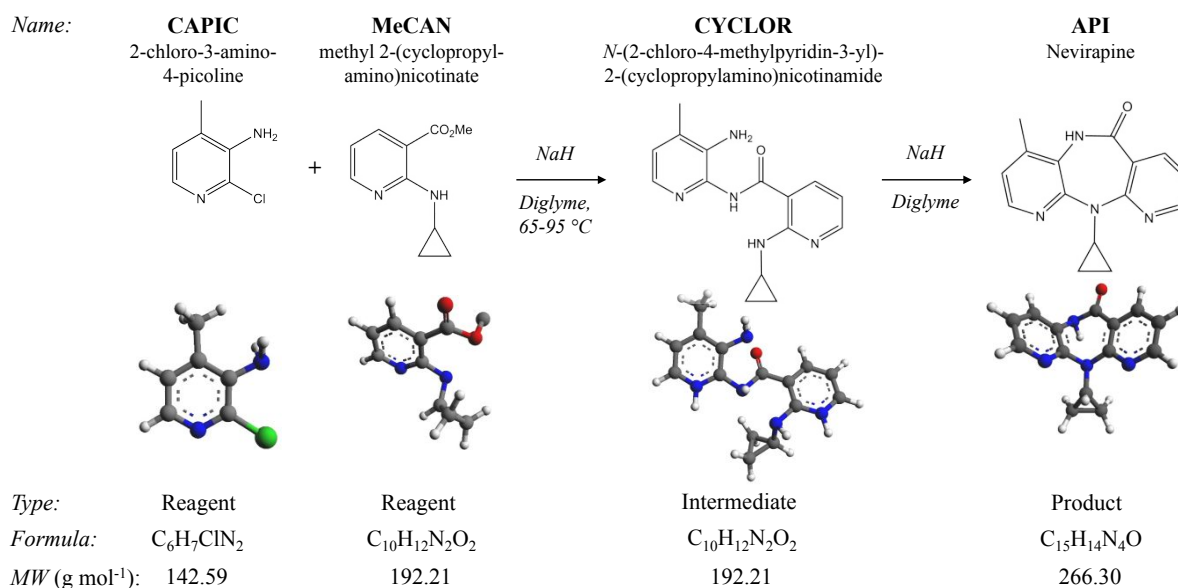**Figure 3**: Nevirapine continuous synthetic strategy from CAPIC and MeCAN.[10]

2.2 Process Flowsheets

Fig. 4 shows the process flowsheet for nevirapine CPM based on the published continuous flow synthesis.[10] The first reactor, R-101, is a thin-film reactor operated at 95 °C; reaction between CAPIC (3 M) and NaH (2 M) in diglyme at 95 °C forms the sodium salt of CAPIC (CAPIC-Na) with evolution of H_2 gas and an estimated 100% conversion of CAPIC. The mixture containing CAPIC-Na is added to a stirred tank (R-102, 65 °C) with neat MeCAN (1.05 eq.) with 82.5% conversion of CAPIC-Na to CYCLOR (+ sodium methoxide, $NaCH_3O$) reported. Finally, CYCLOR undergoes ring closure in the presence of a packed bed of NaH (R-103) to form nevirapine (API). The subsequent crystallisation can be performed in batch or continuous mode. Various reaction performances at different temperatures (T_{R103}) are reported in the demonstrated continuous flow synthesis,[10] discussed further in section 2.3.1.3.
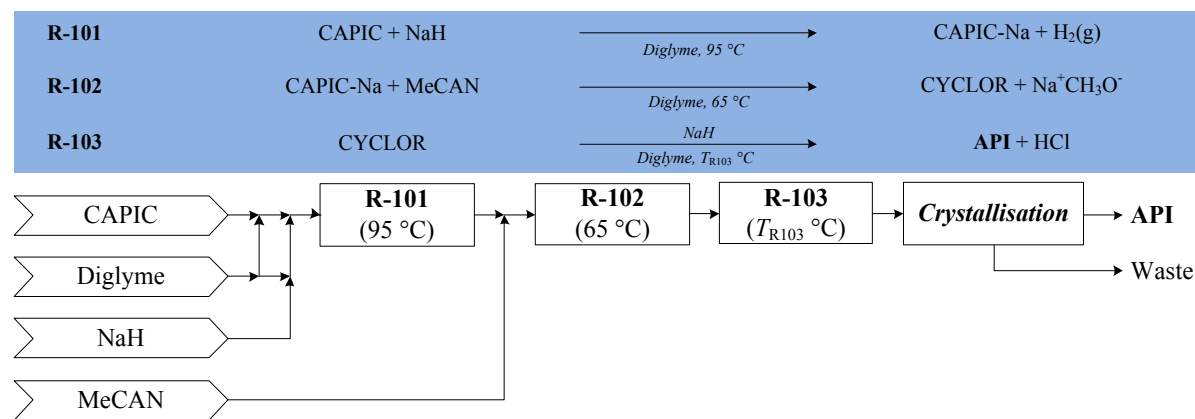

Figure 4: Process flowsheet for the CPM of nevirapine.

The flowsheet for the crystallisation process following the continuous flow synthesis is shown in Fig. 5. The effluent of R-103 is feed to a stirred tank where aqueous HCl is added; the API is more soluble at lower pH in aqueous solutions. Activated carbon (AC) is also added to adsorb organic impurities prior to their subsequent removal via filtration.[10] Nevirapine (API) is then crystallised from solution by decreasing the API solubility by increasing pH by addition of aqueous NaOH solution. The crystallisation following the continuous flow synthesis can be either implemented in batch (BX) or continuous (CPM) mode. Details of crystallisation modelling are provided in section 2.3.2.
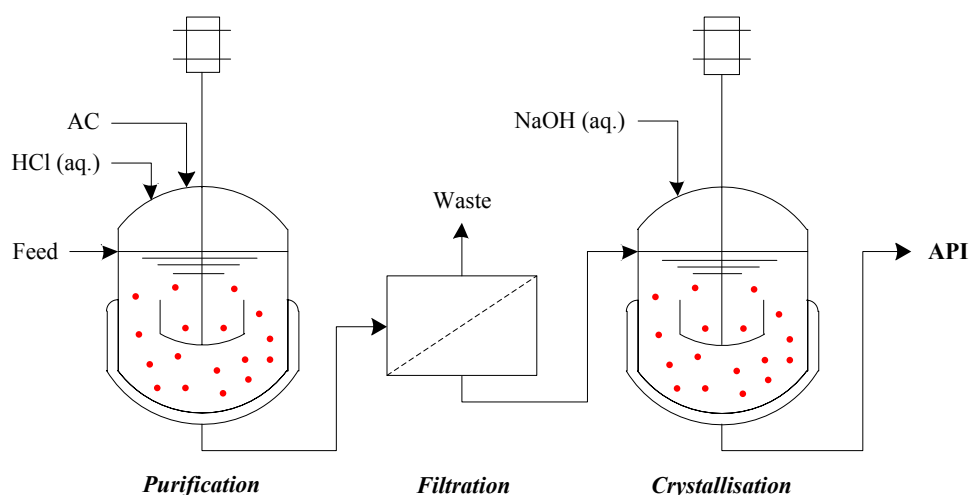

Figure 5: Crystallisation of API operated in batch (BX) or continuous (CPM) mode.[10]

2.3 Modelling and Nonlinear Optimisation
2.3.1 Reactor Design and Kinetic Parameter Estimation
Plantwide mass balances are required for detailed unit operation modelling and plantwide performance analysis. Molar balances across each reactor are calculated via eq. 1.

$$F_i^j = F_{A,0}^j \left(\Theta_i^j + v_i^j X_A^j \right) \tag{1}$$

Here, F_i^j is the molar flowrate of component i exiting reactor j, $F_{A,0}^j$ is the inlet molar flowrate of limiting reagent A in reactor j, Θ_i^j is the molar ratio of component i to limiting reagent A in reactor j, v_i^j is the stoichiometric coefficient of component i in reactor j and X_A^j is the conversion of limiting reagent A in reactor j. Modelling and design of each reactor in the process flowsheet (Fig. 3) is now discussed. Fixed process conditions for each of the three reactors required are summarised in Table 2.

Table 2: Summary of continuous flow reactor conditions used in process modelling.

Reactor	Reaction	Temperature, T (°C)	τ (units)	X_A (%)
R-101	CAPIC + NaH → CAPIC-Na	95	8.56 (s)	100
R-102	CAPIC-Na + MeCAN → CYCLOR	65	2 (hr)	82.5
R-103	CYCLOR → API	Variable	21 (min)	$X_A^{R103} = f(T_{R103})$

2.3.1.1 Reactor R-101
Full conversion of CAPIC to CAPIC-Na ($X_A^{R101} = 100\%$) is reported for a R-101 operating temperature of 95 °C and an estimated residence time of 8.56 s; this stoichiometric conversion in a short residence time is allowed by implementing a thin-film reactor to enhance and heat and mass transfer to expedite the reaction.[10] The operating temperature of R-101 is chosen to be the same as in the published experimental demonstration ($T_{R101} = 95$ °C); thus, the same reaction performance ($X_A^{R101} = 100\%$) is assumed for modelling CAPIC-Na formation in R-101.

2.3.1.2 Reactor R-102
A conversion of CAPIC-Na to CYCLOR of 82.5% is reported for a R-102 operating temperature of $T_{R102} = 65$ °C and an estimated residence time of $\tau = 2$ hr.[10] The operating temperature of R-102 is chosen to be the same as in the published experimental demonstration ($T_{R102} = 65$ °C); thus, the same reaction performance ($X_A^{R102} = 82.5\%$) and residence time ($\tau = 2$ hr) are assumed the same reaction performance is assumed for modelling the CYCLOR formation in R-102.

2.3.1.3 Reactor R-103
Temperature-dependent kinetic data for API formation in R-103 is available in the literature;[10] at temperatures of 120, 140 and 165 °C, CYCLOR conversions to API of 10, 60 and 96% are attainable, respectively, each for an estimated residence time of 21 min.[10] The packed bed reactor (PBR) design equation is provided in eq. 2.

$$\tau_{R103} = C_{A,0} \int_0^{X_A} \frac{dX_A}{-r_A} \tag{2}$$

Here, τ_{R103} is the residence time of R-103, $C_{A,0}$ is the concentration of limiting reagent (CYCLOR) and r_A is the rate of reaction of limiting reagent. The limiting reagent is CYCLOR as NaH in the packed bed is in significant excess and so it is assumed that the reaction is first-order in CYCLOR. Following this assumption, the first-order rate constant, k, at different temperatures can be estimated. This allows the regression of Arrhenius law (eq. 3) parameters, the pre-exponential factor, A, and activation energy, E_a, for API formation in R-103, allowing the explicit modelling of CYCLOR conversion to API as a function of temperature, T

$$k(T) = A\exp\left(-\frac{E_a}{RT}\right) \tag{3}$$

where R is the universal gas constant. The Arrhenius plot from the available kinetic data is shown in Fig. 6 with good fit (coefficient of determination, $R^2 > 0.96$); regressed parameters are E_a = 1.565 kJ mol^{-1} and A = 8.49×10^{13}, assuming R-103 is first-order in CYCLOR. Availability of a wider kinetic dataset will allow further validation of Arrhenius parameter estimation results and investigation of more complex candidate rate law expressions.
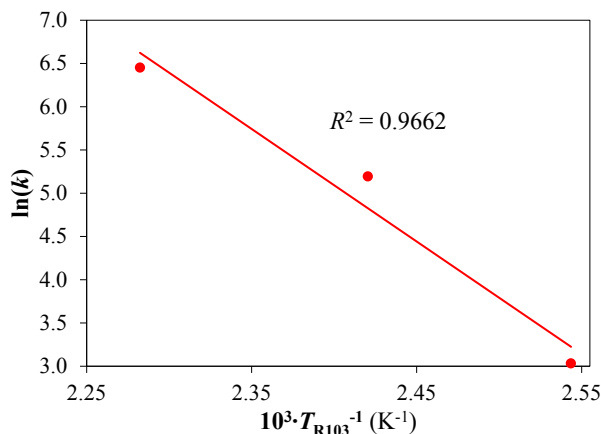

Figure 6: Arrhenius plot for ring closure in the API continuous flow synthesis.

2.3.2 Crystallisation Process

The batch crystallisation yield has a reported yield of 96% in a residence time of 1 hr operating at 25 °C and pH_{CRYST} = 7.[10] Here, we compare the conceptual steady-state continuous crystallisation (CPM) to the demonstrated batch (BX) process by varying the pH of the continuous crystallisation. Table 3 summarises fixed processing conditions for both batch and continuous crystallisation process designs.

Table 3: Summary of fixed process conditions for batch and continuous crystallisation process models.

	Batch (BX)	Continuous (CPM)
Temperature (°C)	25	25
Thermodynamic efficiency (%)	100	70
τ (hr)	1	0.5
Feed pH	≈ 0.5	≈ 0.5
Operating pH, pH_{CRYST}	7	Variable
Yield, Y (%)	96	$Y = f(pH_{CRYST})$

Crystallisation process design requires modelling of API solubility in process mixtures. The mixture prior to pH increase for API crystallisation is predominantly aqueous (solvent content >96 mol% H_2O), thus the mixture is assumed to be purely aqueous for crystallisation modelling purposes. The aqueous solubility, S, of nevirapine in the crystallisation stage (see Fig. 5) as a function of pH is modelled by[38]

$$S = S_0(1 + 10^{pKa-pH}) \tag{4}$$

where S_0 = 4.58×10^{-2} g L^{-1} (solubility under non-ionising conditions) and pK_a = 2.8 at 25 °C;[38] correlation parameter values (S_0 and pK_a) are only available at 25 °C, thus additional temperatures for cooling crystallisation modelling cannot be considered. The modelled aqueous API solubility as a function of pH is shown with experimental values as reported by various literature references in Fig. 7, showing good agreement with experimental values.[38,40,41]
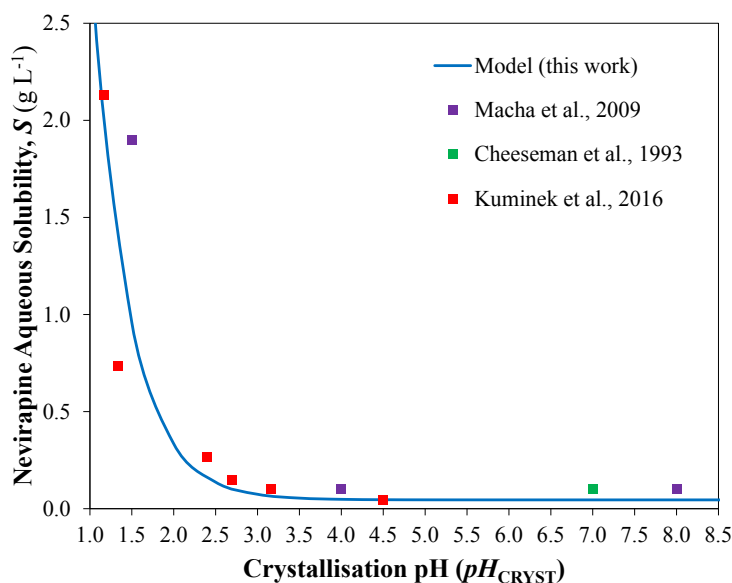
Figure 7: Aqueous API solubility model $= f$ (pH) with experimental values.[38,40,41]

The crystallisation yield (eq. 5) is estimated from the API concentration in the mother liquor, C_{CRYST}, and the aqueous API solubility, S.

$$Y = 1 - \frac{C_{\mathrm{CRYST}}}{S} \tag{5}$$

Both batch and continuous crystallisation processes' feed streams enter at pH ≈ 0.5. A residence time of 0.5 hr is assumed for the continuous crystallisation, chosen to be lower than that of the batch crystallisation to reflect the difference in residence times typical of these different operation modes. It is assumed that the batch crystallisation attains full (100%) thermodynamic equilibrium. A conservative thermodynamic efficiency of 70% is assumed for the continuous crystallisation to account for uncertainty in the assumed residence time and the calculated yield. This will likely result in an under-prediction of continuous crystallisation yield and thus an over-estimation of total costs, which should be considered when interpreting the optimisation results presented here. Provision of detailed crystallisation kinetics for nevirapine as well as dynamic and steady-state crystallisation models for batch and continuous crystallisation processes, respectively, will provide more detailed process design results and insight into the comparative evaluation of batch vs. continuous crystallisation for nevirapine.

2.4 Process Material Efficiencies

Quantities of waste produced by different designs are compared via the popular green chemistry metric, the environmental (E)-factor (eq. 6), defined as the mass ratio of waste to desired product, i.e., recovered API.[42,43] Here, m_{waste} is the total mass of waste, m_{API} and m_{uAPI} are the mass of recovered and unrecovered API, respectively, m_{uS} is the mass of unrecovered solvent and m_{ur} is the mass of unreacted reagents.

$$E = \frac{m_{\mathrm{waste}}}{m_{\mathrm{API}}} = \frac{m_{\mathrm{uAPI}} + m_{\mathrm{uS}} + m_{\mathrm{ur}}}{m_{\mathrm{API}}} \tag{6}$$

2.5 Costing Methodology

2.5.1 Capital Expenditure (CapEx)

We implement an established methodology for costing pharmaceutical manufacturing processes.[5] All plant designs are assumed to be constructed and operated at an existing pharmaceutical manufacturing site with essential auxiliary structures already in place. Annual operation of 8,000 hours is considered. Prices for equipment of similar capacities to those considered here have been sourced where possible; where such data is unavailable, the following cost-capacity correlation is used.[44]

$$P_{\mathrm{B}} = f P_{\mathrm{A}} \left(\frac{S_{\mathrm{B}}}{S_{\mathrm{A}}} \right)^{n} \tag{7}$$

P_{j} is the equipment purchase cost at capacity S_{j}. Parameters n and f are equipment-dependent and found in the literature.[45] Where the reference purchase cost (P_{A}) is taken from the past, chemical engineering plant cost indices (CEPCIs) are used to calculate the corresponding purchase cost in the year 2018. All equipment capacities are scaled to account for plantwide inefficiencies and to meet the specified plant capacity. Unit costs and parameter values for f and n (eq. 7) are given in previous work.[5,46] Unit operations similar to those implemented in the demonstrated continuous flow synthesis[10] were implemented and scaled and costed using published eq. 7 parameters.[45] Table 4 gives details for the purchase costs and scaling parameters in eq. 20 for each equipment item.

Table 4: Parameters for scaled equipment purchase costs (eq. 7).[45]

Item	Ref. Year	Ref. Cost, P_{A} (GBP)	Capacity Basis	Ref. Capacity, S_{A}	n	f (%)
R-101	2007	29,259	Volume (m^3)	3.00	0.53	10.33
R-102	2007	29,259	Volume (m^3)	3.00	0.53	10.33
R-103	2007	273,079	Volume (m^3)	3.00	0.68	10.33
Pump	2015	958	-	-	-	-
Cooler	2015	3,454	-	-	-	-
Mixer	2007	22,230	Power (kW)	5	0.30	10.33
Crystalliser	2007	328,875	Volume (m^3)	10	0.22	10.33

The sum of all inflation-adjusted equipment costs (P_{B}) gives the Free-on-Board (*FOB*) cost. The Chilton method is used to calculate the battery limits installed cost (*BLIC*).[44] The installed equipment cost (*IEC*), process piping and instrumentation (*PPI*) and total physical plant cost (*TPPC*) are calculated from eqs. 8–10. A construction factor of 30% is added to the *TPPC* to calculate the *BLIC* (eq. 11).

$$IEC = 1.43 FOB \tag{8}$$
$$PPI = 0.42 IEC \tag{9}$$
$$TPPC = IEC + PPI \tag{10}$$
$$BLIC = 1.3 TPPC \tag{11}$$

Working capital (*WC*) costs are taken as 35% and 3.5% of annual material costs scaled to meet the desired plant capacity (MAT_{annual}) for batch and continuous processes, respectively (eq. 11). Contingency costs (*CC*) are calculated as 20% of the *BLIC* (eq. 13). The sum of *BLIC*, *WC* and *CC* gives the total capital expenditure (*CapEx*, eq. 14).

$$WC = \begin{cases} 0.350 MAT_{\mathrm{annual}}, \text{batch} \\ 0.035 MAT_{\mathrm{annual}}, \text{CPM} \end{cases} \tag{12}$$
$$CC = 0.2 BLIC \tag{13}$$
$$CapEx = BLIC + WC + CC \tag{14}$$

2.5.2 Operating Expenditure (OpEx)

Required material prices are summarised in Table 5. Base case prices for starting materials CAPIC and MeCAN are assumed in this work. Current lab-scale demonstrations of batch syntheses of these starting materials estimate prices of CAPIC and MeCAN to be higher;[10] however, these estimations are made from batch synthesis material requirements using reagent grade materials. Given the larger scales of operation considered in this work, it can be assumed that material prices will be lower. The annual utilities cost ($UTIL_{\mathrm{annual}}$) is calculated as 0.96 GBP kg^{-1} of process material throughput (m_{process}) + the utilities costs for heating R-103. The heating duty for R-103 is assumed to be the sensible heat required to heat the process stream from $T_{\mathrm{R102}} = 65$ °C to T_{R103}, assuming a heat loss of 20% and an electricity

cost of 13.86 p kWh^{-1}; assuming heat loss of 20% is a rather high estimate for the process scales considered here, thus over-estimates in utilities cost values may be present. The annual waste cost ($Waste_{annual}$) is 0.35 GBP L^{-1} of waste (Q_{waste}). Annual operating expenditure ($OpEx_{annual}$) is the sum of annual material, utilities and waste costs.

$$UTIL_{annual} = 0.96m_{process} + 0.1386Q_{R103} \tag{15}$$
$$Waste_{annual} = 0.35Q_{waste} \tag{16}$$
$$OpEx_{annual} = MAT_{annual} + UTIL_{annual} + Waste_{annual} \tag{17}$$

Table 5: Material prices for reagents and components used in continuous API synthesis and crystallisation.

Type	Material	Price (GBP kg^{-1})	Type	Material	Price (GBP kg^{-1})
Synthesis	CAPIC	5.00	Crystallisation	AC	1.50
	Diglyme	3.00		HCl (aq.)	0.50
	MeCAN	10.00		NaOH (aq.)	0.25
	NaH	5.00			

2.5.3 Total Costs

The total cost of the plant designs is calculated as the sum of *CapEx* and the sum of inflation-adjusted $OpEx_{annual}$ over the plant lifetime (eq. 18).

$$Total\ Cost = CapEx + \sum_{j=1}^{t=20} \frac{OpEx_{annual}}{(1+y)^j} \tag{18}$$

A plant-operating lifetime of $t = 20$ yr and an interest rate of $y = 5\%$ are considered. All *CapEx* is assumed to occur in year 0 and operation is assumed to begin in year 1. Annual operation of 8,000 hours per year is assumed for consistency with our previously published work in this field. The assumed annual operation time can easily be altered to account for varying asset utilisation efficiencies in the presented modelling framework by an expert reader.

2.6 Nonlinear Optimisation Formulation

The objective of the optimisation problem is to minimise plantwide total costs (eq. 19). The continuous decision variables are the operating temperature of R-103, T_{R103}, and crystallisation pH, pH_{CRYST}, both of which influence the final API yield by influencing R-103 conversion to API and crystallisation yield, respectively. While increasing T_{R103} enhances the conversion of CYCLOR to API, there are associated utilities costs with heating R-103 (eq. 15), which contribute to *OpEx* and plant total costs. Similarly, while increasing pH_{CRYST}, the crystallisation pH increases, but also incurs higher material costs as well as larger crystallisation capacities, which contribute to total costs.

Constraints on R-103 operating temperature are chosen to be the lower and upper bounds of available temperature data for Arrhenius parameter estimation (120 and 165 °C, respectively) to ensure validity of the regressed parameters for subsequent modelling and optimisation (eq. 20). Constraints on crystallisation pH (eq. 21) were chosen to be from $pH_{CRYST} = 1$ (close to feed mixture point, pH ≈ 0.5) and pH = 7 (the BX crystallisation pH).

$$\min\ Total\ Cost \tag{19}$$
s.t.

$$120\ °C \leq T_{R103} \leq 165\ °C \tag{20}$$
$$1 \leq pH_{CRYST} \leq 7 \tag{21}$$

The optimisation problem is solved in MATLAB using the interior-point algorithm with tolerances of 10^{-6}. Plant capacities of $Q_{API} = \{10^2, 10^3\}$ kg API yr^{-1} are investigated to represent small-/pilot-scale designs and to be consistent with our previous publications.[5,46–48] The effect of solvent recovery, *SR*, is also considered, as this has a significant effect on material consumption, and thus material cost

contributions towards *OpEx*. A reported solvent recovery of 80% is reported in the literature;[10] the attainable *SR* may be lower in practice; lower values of 0 and 40% are also considered in this work.

The nonlinear optimisation problem was solved for all individual combinations of plant capacity, Q_{API} = {10^2, 10^3} kg API yr^{-1} and assumed solvent recovery, *SR* = {0, 40, 80}%, i.e. six problem instances, to avoid mixed integer problem formulations and reduce optimisation problem complexity. Multiple initial values for decision variables are tested to ensure a unique optimal solution for each problem instance. Initial values of decision variable for each problem instance are R-103 temperature, $T_{R103,0}$ = {130, 145, 160} °C and crystallisation pH, $pH_{CRYST,0}$ = {2, 4, 6}, i.e. a total of nine initial points per problem instance. Unique solutions were attained for all problem instances for different decision variable initial values. Solution times were short for all problem instances (Table 6).

Table 6: Optimisation problem solution time for different problem instances.

Q_{API} (kg API yr^{-1})	*SR* (%)	Solution time (s)
	0	14.5
10^2	40	19.5
	80	7.8
	0	8.7
10^3	40	7.5
	80	7.4

3. Results and Discussion

3.1 Total Cost Response Surfaces and Optimal Operating Conditions

Cost response surfaces under different design assumptions were generated (presented in Fig. 8) to investigate the design space and to ensure that multiple cost minima are not present. Cost response surfaces for all design cases show a sharp peak (i.e. very high total costs) at low R-103 operating temperature T_{R103} and low crystallisation pH (pH_{CRYST}). Under these conditions, very low API recovery is attained and thus higher material requirements and unit operation capacities are required to meet the desired plant capacity (Q_{API}), resulting in high *CapEx* and *OpEx*. At higher capacity (Q_{API}), response surfaces take a similar shape but present higher total cost values due to the increased material throughput and correspondingly larger unit operation scales. Varying solvent recovery is also shown to significantly affect the cost response surfaces due to its effect on solvent requirements, which is a major contributor to the mixture composition and thus on *OpEx* components, as well as waste.

Optimal decision variables (R-103 operating temperature, T_{R103}, crystallisation pH, pH_{CRYST}) corresponding to minimum total costs under different design assumptions are shown in Fig. 9. These optima are compared to the process implementing a batch (BX) crystallisation where T_{R103} = 165 °C and pH_{CRYST} = 7). In all BX and CPM design cases, T_{R103} is at the upper bound of 165 °C. The optimum crystallisation pH varies across different CPM design assumptions. At lower solvent recovery (*SR* = 0%), optimum pH ≈ 4 is observed for both considered capacities; at low *SR*, *OpEx* components are significant contributors to total costs and thus higher crystallisation yields are preferred to lower total costs. For higher *SR* = {40, 80}%, pH is driven to the lower bound of 1; the effect of enhancing crystallisation yield by increasing pH_{CRYST} is not as important when significant solvent is recovered and T_{R103} is high. At higher capacity (Q_{API} = 10^3 kg API yr^{-1}), higher solvent recovery is required to allow a lower pH at cost optima. In industrial practice, it may be necessary to neutralise the mixture following crystallisation and API crystal removal for safety purposes, however this is not considered as part of the presented analysis.

The effect of R-103 operating temperature (T_{R103}) on total costs is significant; total costs decrease rapidly as T_{R103} increases from 125 to 165 °C (Fig. 8). Operating temperature in R-103 significantly affects the conversion of CYCLOR to API, thus plantwide API yield is very sensitive to T_{R103}; expensive reagents, especially starting materials CAPIC and MeCAN, make materials costs a major contributor to total costs and so a high API yield in R-103 (i.e. high T_{R103}) is preferred. The effect of each decision variable (T_{R103} and pH_{CRYST}) on plantwide API yield is shown in Fig. 10 to illustrate this point. The optimisation problem formulation in this work could alternatively be defined to maximise net present value (NPV), which may yield different results. However, problem formulation for NPV maximisation requires the estimation of product sales revenues, which will vary with design assumption (see section 3.3 for estimated API cost of goods for different plant designs). For this reason, the objective is instead

to minimise plant total costs. Comparison of results for a different objective function formulation could be useful, given the availability of reliable projected API and brand sales prices.

The effect of operating crystallisation pH (pH_{CRYST}) on total costs is also similar across different design assumptions (Fig. 8). At the lower bound of R-103 operating temperature ($T_{R103} = 125$ °C), low pH (e.g., at the lower bound of $pH_{CRYST} = 1$) results in high total costs. At low T_{R103}, the low conversion of CYCLOR to API in R-103 means plantwide yield is already poor prior to crystallisation; low pH_{CRYST} implies lower crystallisation yield and thus higher total costs are incurred due to increased material requirements and unit operation scales needed to meet the desired plant capacity (Q_{API}). The implemented model of aqueous API solubility vs. pH (eq. 4, Fig. 7) shows a plateau in solubility beyond some pH value below 7. Increasing the crystallisation pH too high will result in incremental increases in API yield at best (as shown in Fig. 10) which will unnecessarily increase material usage and crystallisation volumes, and thus total costs (as observed in the cost response surfaces in Fig. 8). At the upper bound of R-103 operating temperature ($T_{R103} = 165$ °C), the effect of crystallisation pH is not so significant. The yield of API is already high when T_{R103} is higher (due to increased conversion of CYCLOR to API in R-103) and thus the effect of higher pH in the crystallisation is not so important. This point is also further illustrated by the plantwide API yield response surface in Fig. 10.
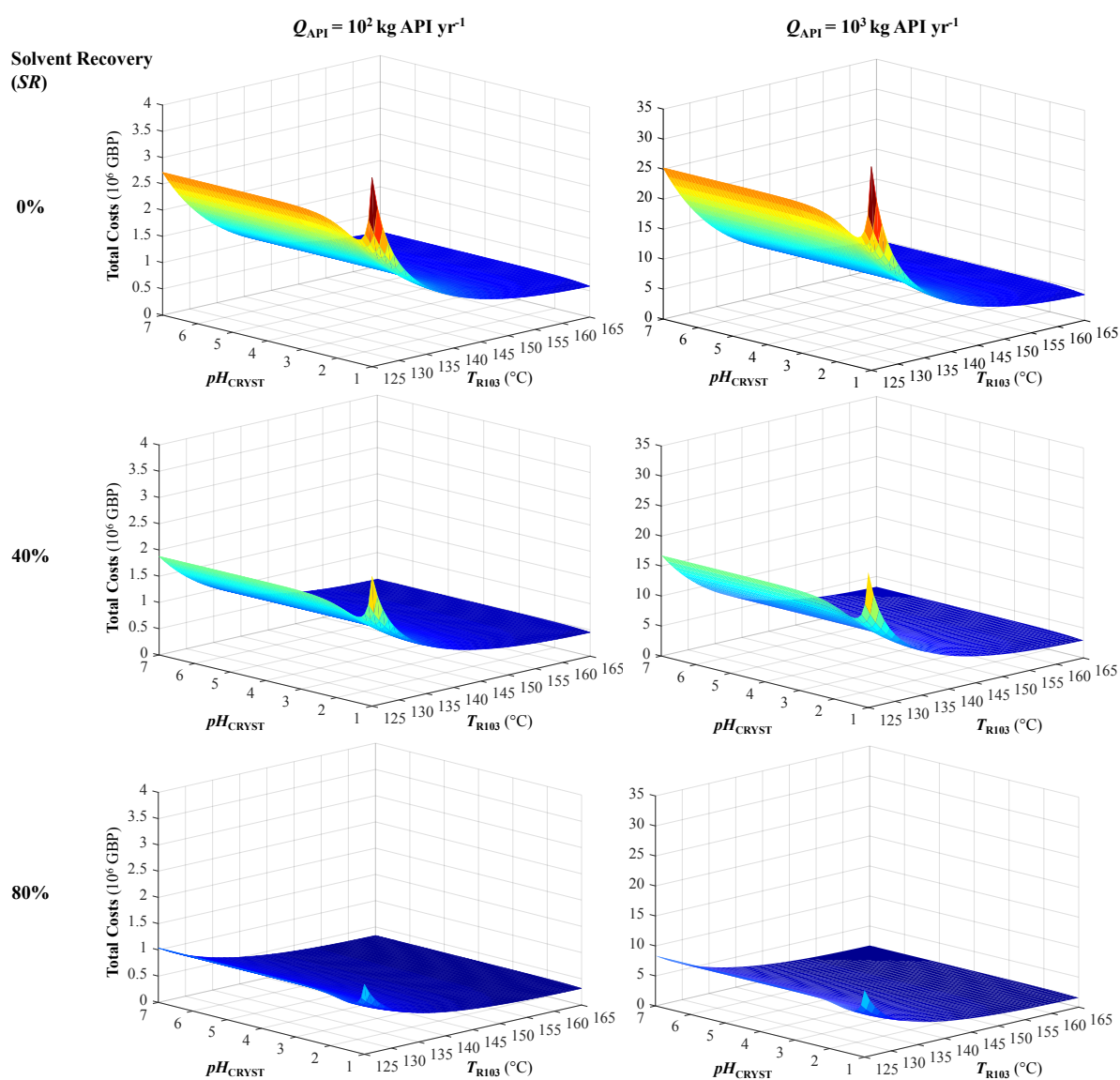

Figure 8: Total cost response surfaces for nevirapine CPM under different design assumption of plant capacity (Q_{API}) and solvent recovery (SR).
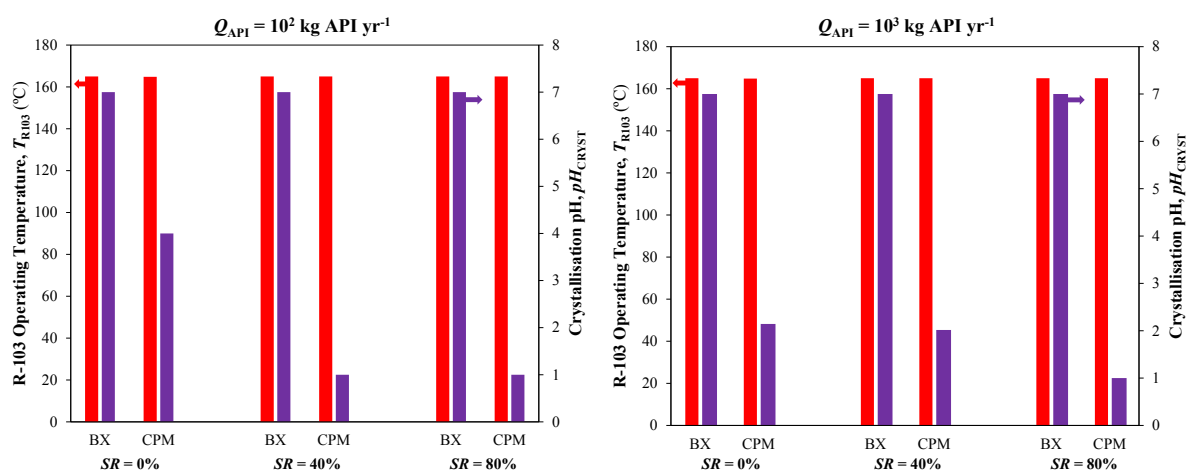
Figure 9: Optimal operating (decision) variables corresponding to total cost minima under different design assumptions.

The current work only optimises the process implementing a continuous crystallisation (CPM) and does not optimise the batch (BX) process. Optimisation of the batch process with respect to decision variables considered here (T_{R103} and pH_{CRYST}) as well as batch scheduling and numbering can allow a fairer comparison to CPM designs and should be implemented in future work.[49] Furthermore, implementation of Process Analytical Technology (PAT) is essential for the success of CPM technologies and ensuring operating (decision) variables do not deviate from their optimal values to ensure minimum total costs, with recent studies have illustrating the importance of PAT in crystallisation applications.[50]
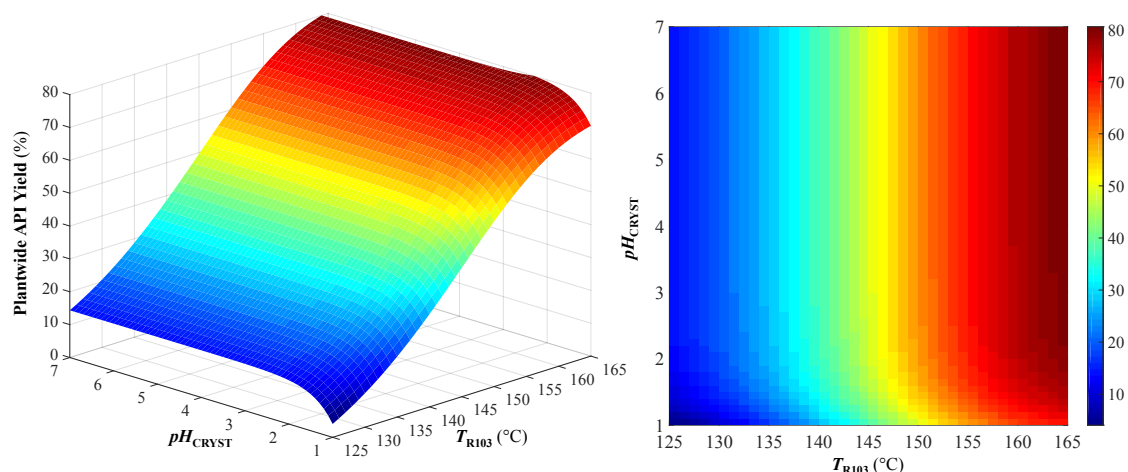

Figure 10: Response surface of plantwide API yield vs. R-103 operating temperature (T_{R103}) and crystallisation pH (pH_{CRYST}).

3.3 Material Efficiencies

Material efficiencies of different design assumptions quantified by the *E*-factor (eq. 5) are shown in Fig. 11. For all batch designs, *E*-factor values are very high, even for pharmaceutical processing which is renowned for having highly materially intensive manufacturing routes;[51] this is due to all batch crystallisation processes being operating at $pH_{CRYST} = 7$, requiring significant quantities of base to neutralise the feed mixture. In all cases, increasing solvent recovery significantly reduces *E*-factor due to the large contribution of solvent to process mixture and waste compositions. For pharmaceutical manufacturing, the *E*-factor can be as high as 200; all CPM designs achieve values lower than this, but only higher solvent recoveries allow this for the process with a batch crystallisation. Elucidation of

attainable solvent recoveries at different production scales will further clarify the likely material efficiencies of different design assumptions to elucidate materially efficient CPM plant designs.
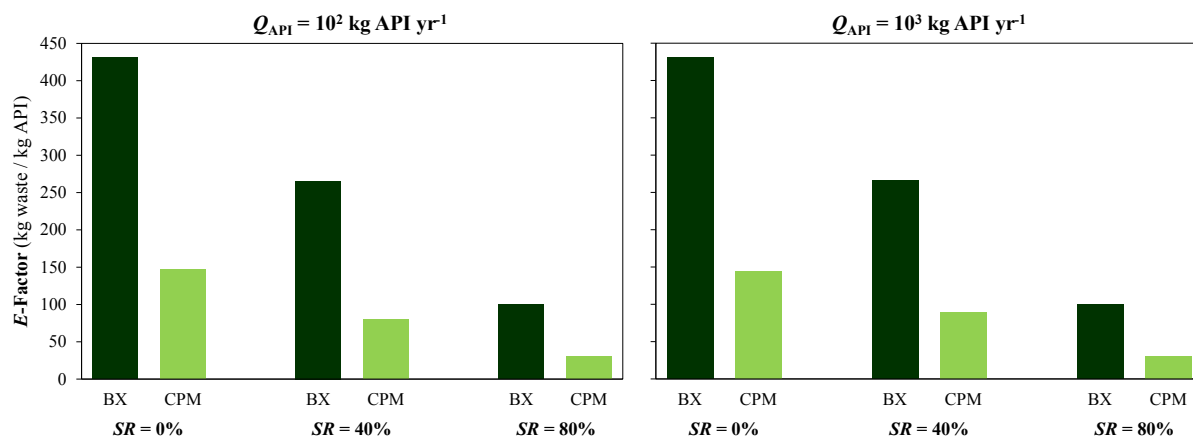

Figure 11: Environmental (*E*)-factors at cost optima for different design assumptions.

3.4 Total Cost Components and API Cost of Goods

Minimum total cost components for CPM are compared the process with the BX crystallisation are compared in Fig. 12 (see also Appendix A, Table A1). Total costs at $Q_{API} = 10^3$ kg API yr^{-1} are higher, reflecting the increased material requirements and unit operation scales. *OpEx* components are more significant than *CapEx* in all design cases due to the expensive reagents required for the API synthesis. As solvent recovery increases, *OpEx* components decrease significantly and substantially lower total costs. Utilities and waste components are the most significantly affected by varying solvent recovery due to the large quantity of solvent in the process mixture; materials costs are less affected by varying solvent recovery as the reagents used are much more expensive than solvent components in the considered process (see Table 2). In all cases, CPM designs have significantly lower *OpEx* components than for BX designs due to the reduced material requirements of the crystallisation process when operating at lower pH. The costing methodology implemented here does not include labour requirements, which are location- and scale-dependent; elucidation of labour costs will further inform process development.
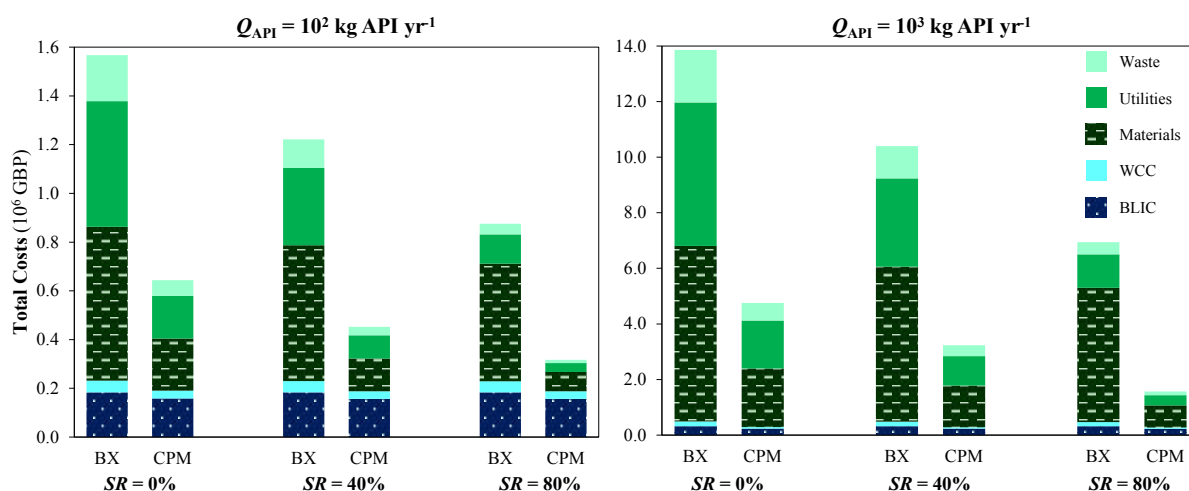

Figure 12: Total cost components for different design assumptions.

For varying solvent recovery assumptions, *CapEx* components remain roughly the same, as internal process stream flowrates through each unit operation remain fairly consistent. In all cases, CPM designs have lower *CapEx* components than their BX counterparts due to the lower material throughputs of these processes. The availability of detailed crystallisation kinetic models with experimental data and

model parameters can further elucidate crystallisation process performance and unit operation design, which will likely have a significant effect on *CapEx*. The equipment cost correlation used here (eq. 7) is the most widely implemented and reliable available in the peer-reviewed literature; design capacities required for the considered plant capacities (Q_{API}) are at the lower end of the cost correlation application range, and thus purchase cost overestimation may be present. Additional uncertainty in calculated unit purchase costs is present due to the lack of cost estimation methods for specific equipment; however, the cost correlation used here is the best available in the literature. The correlation is the most widely implemented in the literature for scaling equipment purchase costs vs. capacity for different types of chemical engineering unit operations. Some specialised unit operations have specific cost correlations established,[52] which may be more accurate than the general correlation used in this work. Cost correlations specific to particular unit operations should be used where possible to allow accurate prediction of *CapEx* component contributions to total costs. Furthermore, the considered processes (both BX and CPM) are considered to take advantage of being constructed at an existing pharmaceutical manufacturing site; additional costs may also be incurred if green-field construction is required.

The starting materials (CAPIC and MeCAN) for the continuous synthesis of nevirapine considered in this work are advanced compounds synthesised from multistep batch processes.[10] Consideration of key material price fluctuations is an important form of sensitivity analysis that should be implemented in modelling and economic evaluation during candidate process screening and development stages.[5] Here, we consider the effect of increasing CAPIC and MeCAN material prices by 50% from the base case values (Table 2) on plant total costs, i.e. CAPIC price = [5,10] GBP kg^{-1}, MeCAN price = [10,20] GBP kg^{-1}, at discrete values of decision variables, T_{R103} = {130, 145, 160} °C and pH_{CRYST} = {2, 4, 6} for Q_{API} = 10^2 kg API yr^{-1} and SR = 40%; observed trends are expected to be the same for alternative values of Q_{API} and SR. The effects of varying material prices for these discrete decision variable values are shown in Fig. 13. Although starting material prices do affect total plant costs in all design cases, the effect of T_{R103} is still the most sensitive parameter affecting total costs. Further process intensification for the batchwise syntheses of CAPIC and MeCAN will ensure reasonable material prices to ensure the economic viability of the process designs investigated here.
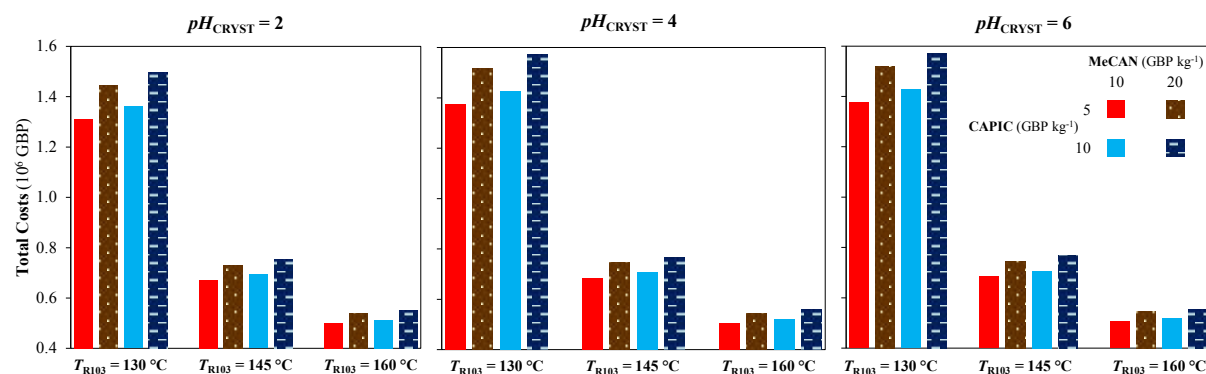

Figure 13: Effect of starting material prices and T_{R103} and pH_{CRYST} on plant total costs (Q_{API} = 10^2 kg API yr^{-1}, SR = 40%).

3.5 API Cost of Goods

In all cases, CPM designs are more economically-viable than those implementing a BX crystallisation. Cost component savings for each process with respect to the corresponding BX design is shown in Table A1 (Appendix A). The most significant savings are realised in *OpEx* components (materials, utilities and waste components, as described in the costing methodology), which allow significant total savings due to their large contribution to plant total costs. Ensuring affordable, accessible HIV medicines is essential; HIV drug unit prices have varied widely in previous years, so quantifying attainable price per unit mass is an important consideration for HIV drug manufacturing.[53] The cost of goods (*CoG*) of API is calculated to quantitatively compare differences in affordability of nevirapine under different design assumptions. The *CoG* is calculated as the total mass of API produced during the plant lifetime divided by the total cost of constructing and operating the plant.

$$CoG \ = \ \frac{Q_{\text{API}}t}{Total\ Costs} \qquad (22)$$

The resulting API *CoG* values under different design assumptions are presented in Fig. 14. For all cases, CPM designs allow lower API *CoG* than their batch (BX) alternatives due to the significant total cost savings allowed by continuous operation. Solvent recovery has a significant effect on the resulting *CoG* due to the large contribution of solvent to *OpEx* components, which dominate total costs of all design cases. While this analysis does not clarify exactly what price the API will be sold at, the estimated *CoG* values indicate that CPM implementation can allow for lower API sales prices to expand global access to this societally-important HIV drug.
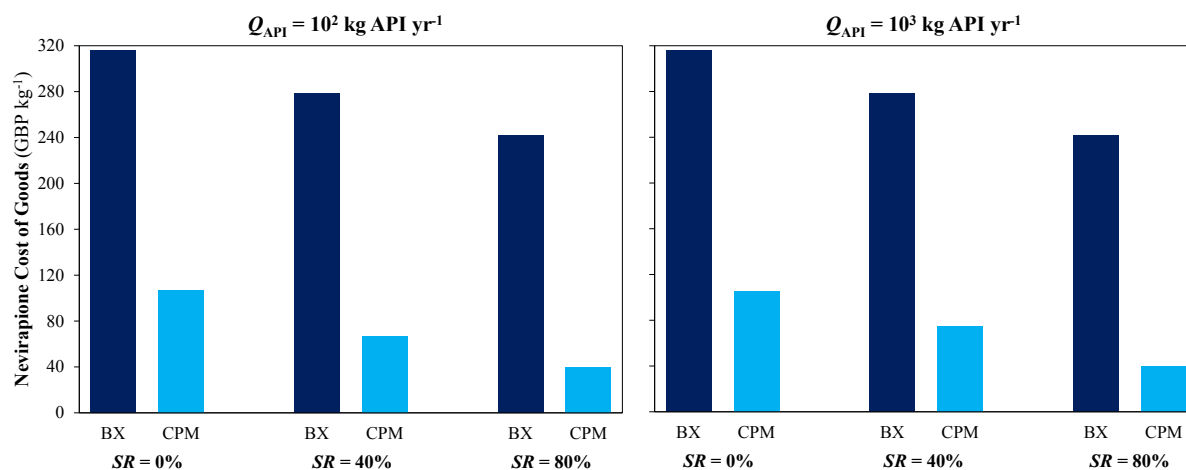

Figure 14: Estimated API cost of goods from total costs of different plant designs.

4. Conclusions

This paper presents the formulation and solution of a nonlinear optimisation problem[54] for the total cost minimisation of plantwide CPM of nevirapine, a societally important API for HIV-1 treatment. Optimisation of a conceptual continuous crystallisation for the purification of the API synthesis effluent following the continuous flow synthesis under various design assumptions (plant capacity and solvent recovery) are used to quantitatively evaluate different designs for atropine CPM. The operating temperature of the final reactor R-103 (T_{R103}) is driven to the upper bound in all design cases to maximise API synthesis yield while crystallisation pH (pH_{CRYST}) is always lower than that of the batch crystallisation (pH = 7) for CPM designs to minimise major *OpEx* contributions to plant total costs. In all design cases, CPM designs achieve lower total cost components, improved material efficiencies and lower API *CoG* values, demonstrating the promise of CPM over batch for nevirapine production and improving global, affordable access to HIV APIs. This work also demonstrates the value of conducting technoeconomic optimisation studies towards the development of continuous processes in pursuit of economically viable end-to-end CPM plants.

Author Information
Corresponding Author
Email: *D.Gerogiorgis@ed.ac.uk*
Phone: *+ 44 131 6517072*

ORCID
Dimitrios I. Gerogiorgis: 0000-0002-2210-6784

Notes
The authors declare no competing financial interest. Tabulated and cited literature data suffice for reproduction of all original process simulation and optimisation results and no other supporting data are required to ensure reproducibility.

Acknowledgements

Appendix A: Total cost components and cost savings

Table A1 details total cost optima component values for both BX and CPM designs and CPM savings with respect to BX crystallisation implementation.

Table A1: Total cost components (10^6 GBP) and CPM savings with respect to BX (%).

	$Q_{API} = 10^2$ kg API yr^{-1}								
	SR = 0%			**SR = 40%**			**SR = 80%**		
	BX	CPM	Savings	BX	CPM	Savings	BX	CPM	Savings
BLIC	0.183	0.159	−13.52	0.183	0.157	−14.64	0.183	0.157	−14.64
WCC	0.048	0.032	−32.76	0.046	0.032	−32.06	0.045	0.031	−30.32
CapEx	0.231	0.191	−17.49	0.230	0.188	−18.16	0.229	0.188	−17.74
Materials	0.632	0.214	−66.18	0.557	0.134	−75.98	0.483	0.079	−83.60
Utilities	0.516	0.175	−66.03	0.318	0.096	−69.94	0.120	0.037	−69.61
Waste	0.189	0.064	−66.03	0.116	0.035	−69.94	0.044	0.013	−69.61
OpEx	1.336	0.453	−66.10	0.992	0.264	−73.33	0.647	0.129	−80.05
Total Costs	1.567	0.644	−58.93	1.221	0.453	−62.95	0.876	0.317	−63.78

	$Q_{API} = 10^3$ kg API yr^{-1}								
	SR = 0%			**SR = 40%**			**SR = 80%**		
	BX	CPM	Savings	BX	CPM	Savings	BX	CPM	Savings
BLIC	0.320	0.235	−26.51	0.320	0.235	−26.58	0.320	0.229	−28.46
WCC	0.174	0.051	−70.95	0.161	0.050	−69.31	0.148	0.047	−68.25
CapEx	0.494	0.286	−42.20	0.481	0.284	−40.92	0.468	0.276	−41.08
Materials	6.316	2.109	−66.62	5.573	1.491	−73.24	4.830	0.792	−83.60
Utilities	5.160	1.730	−66.47	3.181	1.065	−66.51	1.202	0.365	−69.61
Waste	1.886	0.632	−66.47	1.162	0.389	−66.50	0.438	0.133	−69.61
OpEx	13.362	4.471	−66.54	9.916	2.946	−70.29	6.470	1.291	−80.05
Total Costs	13.856	4.757	−65.67	10.397	3.230	−68.93	6.939	1.567	−77.42

Nomenclature and Acronyms

Acronyms

API	Active pharmaceutical ingredient
BX	Batch
CEPCI	Chemical engineering plant cost index
CPM	Continuous pharmaceutical manufacturing
HIV	Human immunodeficiency virus
LLE	Liquid-liquid extraction
NPV	Net present value
PAT	Process analytical technology
PBR	Packed bed reactor
WHO	World Health Organisation

Variables

Latin Letters

A	Pre-exponential factor
BLIC	Battery limits installed costs (GBP)

C_{CRYST}	Concentration of API in the crystallisation mother liquor (g L^{-1})	
$C_{i,0}$	Initial concentration of reagent i (M)	
$CapEx$	Capital expenditure (GBP)	
CC	Contingency costs (GBP)	
CoG	Cost of goods (GBP kg^{-1})	
E	Environmental (E)-factor	
E_a	Activation energy (J mol^{-1})	
f	Correction factor in eq. 7	
$F_{A,0}^{j}$	Molar flowrate of limiting reagent A entering reactor j (mol s^{-1})	
F_i^{j}	Molar flowrate of component i exiting reactor j (mol s^{-1})	
FOB	Free-on-Board Costs (GBP)	
IEC	Installed equipment costs (GBP)	
k	1st-order reaction rate constant of R-103 (s^{-1})	
m_{API}	Mass of recovered API (kg yr^{-1})	
$m_{process}$	Plant material throughput (kg yr^{-1})	
m_{ur}	Mass of reagents remaining in waste streams (kg yr^{-1})	
m_{uAPI}	Mass of unrecovered API (kg yr^{-1})	
m_{uS}	Mass of unrecovered solvent (kg yr^{-1})	
m_{waste}	Mass of waste (kg yr^{-1})	
MAT_{annual}	Annual material costs (GBP yr^{-1})	
n	Exponent in eq. 7	
$OpEx_{annual}$	Annual operating expenditure (GBP yr^{-1})	
P_j	Equipment purchase cost at capacity j (GBP)	
pH_{CRYST}	Crystallisation pH	
$pH_{CRYST,0}$	Initial value of crystallisation pH in problem formulation	
PPI	Process piping and instrumentation costs (GBP)	
Q_{API}	Plant API capacity (kg API yr^{-1})	
Q_{R103}	Heating duty of R-103 considering 20% heat loss	
Q_{waste}	Volumetric flow of waste output (L yr^{-1})	
R	Universal gas constant (8.314 J mol^{-1} K^{-1})	
R^2	Coefficient of determination	
S	Aqueous API solubility (g L^{-1})	
S_j	Capacity of equipment j (varying units)	
S_0	Non-ionised aqueous API solubility (g L^{-1})	
SR	Solvent recovery (%)	
T_i	Operating temperature of reactor i (°C)	
$T_{R103,0}$	Initial value of R-103 operating temperature (°C) in problem formulation	
t	Plant operation lifetime (yr)	
$TPPC$	Total physical plant cost (GBP)	
$UTIL_{annual}$	Annual utilities costs (GBP yr^{-1})	
V_j	Volume of unit j (m^3)	
$Waste_{annual}$	Annual waste disposal cost (GBP yr^{-1})	
WC	Working capital costs (GBP)	
X_A^{j}	Conversion of limiting reagent in reactor j (%)	
Y	Crystallisation yield (%)	
y	Interest rate (%)	

Greek Letters

Θ_i^{j}	Molar ratio of excess reagent i to limiting reagent in reactor j
ν_i^{j}	Stoichiometric coefficient of reagent i in reactor j
τ	Residence time (s)

Molecules and Reagents

2-CAN	2-(cyclopropylamino)nicotinic acid
AC	Activated carbon

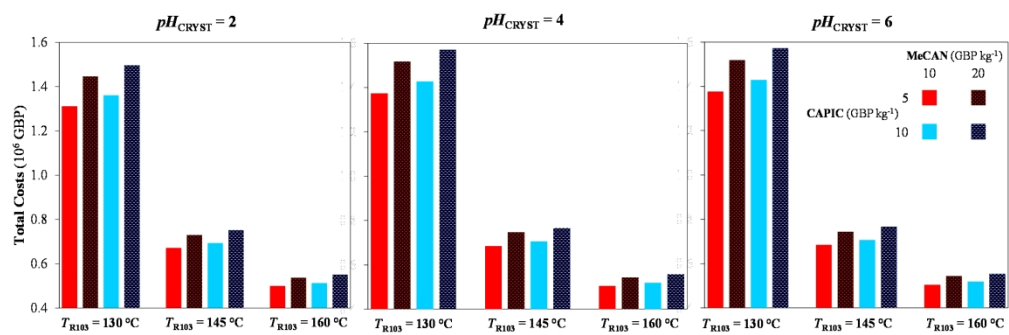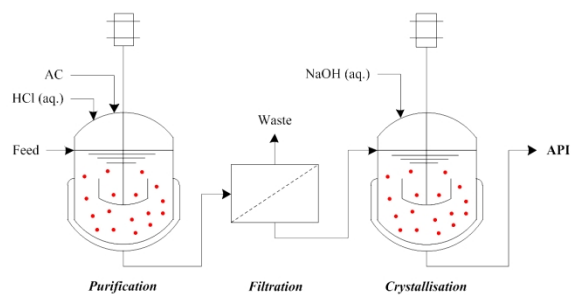| Ac$_2$O | Acetic anhydride |
Al$_2$O$_3$	Aluminium oxide
API	Active pharmaceutical ingredient (Nevirapine)
CAPIC	2-chloro-3-amino-4-picoline
CAPIC-Na	CAPIC sodium salt
COMAD	2-chloro-4-methylnicotinamide
CPA	Cyclopropylamine
CYCIC	2-chloro-4-methylnicotinonitrile
CYCLOR	*N*-(2-chloro-4-methylpyridin-3-yl)-2-(cyclopropylamino)nicotinamide
DMF-DMS	Dimethyl formamide-dimethyl sulphate
H$_2$SO$_4$	Sulphuric acid
HCl	Hydrogen chloride
IPA	Isopropyl alcohol
KOH	Potassium hydroxide
MeCAN	2-(cyclopropylamino)nicotinate
MeOH	Methanol
Mg$_2$SO$_4$	Magnesium sulphate
NaH	Sodium hydride
NaOBr	Sodium hypobromite
NaOH	Sodium hydroxide
PhMe	Toluene
SOCl$_2$	Thionyl chloride
TEA	Triethylamine

References

1. Fortunak, J.M.; de Souza, R.O.M.A.; Kulkarni, A.A.; King, C.L.; Ellison, T.; Miranda, L.S.M., Active pharmaceutical ingredients for antiretroviral treatment in low- and middle-income countries: a survey. *Antivir. Ther.* **2014**, *19*(3): 15–29.

2. UNAIDS, 2018, Data 2018.

3. World Economic Forum, 2017, The global competitiveness report 2017/2018.

4. Dallinger, D.; Kappe, C.O., Why flow means green – Evaluating the merits of continuous processing in the context of sustainability. *Curr. Opin. Green Sust. Chem.* **2017**, *7*: 6–12.

5. Jolliffe, H.G.; Gerogiorgis, D.I., Plantwide design and economic evaluation of two continuous pharmaceutical manufacturing (CPM) cases: ibuprofen and artemisinin. *Comput. Chem. Eng.* **2016**, *27*: 927–932.

6. de Souza, R.O.M.A.; Watts, P., Flow processing as a tool for API production in developing economies. *J. Flow Chem.* **2017**, *7*(3): 146–150.

7. Gérardy, R.; Emmanuel, N.; Toupy, T.; Kassin, V.E.; Tshibalonza, N.N.; Schmitz, M.; Monbaliu, J.C.M., Continuous flow organic chemistry: successes and pitfalls at the interface with current societal challenges. *Eur. J. Org. Chem.* **2018**, 20: 2301–2351.

8. Britton, J.; Raston, C.L., Multi-step continuous-flow synthesis. *Chem. Soc. Rev.* **2017**, *52*(5): 10159–10162.

9. Baxendale, I.R.; Braatz, R.D.; Hodnett, B.K.; Jensen, K.F.; Johnson, M.D.; Sharratt, P.; Sherlock, J.P.; Florence, A.J., Achieving continuous manufacturing: technologies and approaches for synthesis, workup, and isolation of drug substance. *J. Pharm. Sci.* **2015**, *104*(3): 781–791.

10. Verghese, J.; Kong, C.J.; Rivalti, D.; Yu, E.C.; Krack, R.; Alcázar, J.; Manley, J.B.; McQuade, D.T.; Ahmad, S.; Belecki, K.; Gupton, B.F., Increasing global access to the high-volume HIV drug nevirapine through process intensification. *Green Chem.* **2017**, *19*(13): 2986-2991.

11. Longstreet, A.R.; Opalka, S.M.; Campbell, B.S.; Gupton, B.F.; McQuade, D.T., Investigating the continuous synthesis of a nicotinonitrile precursor to nevirapine. *Beilstein J. Org. Chem.* **2013**, *9*:

2570–2578.

12. Longstreet, A.R.; Campbell, B.S.; Gupton, B.F.; McQuade, D.T., Improved synthesis of mono- and disubstituted 2-halonicotinonitriles from alkylidene malononitriles. *Org. Lett.* **2013**, *15*(20): 5298–5301.

13. Teoh, S.K.; Rathi, C.; Sharratt, P., Practical assessment methodology for converting fine chemicals processes from batch to continuous. *Org. Process Res. Dev.* **2015**, *20*(2): 414–431.

14. Bana, P.; Örkényi, R.; Lövei, K.; Lakó, Á.; Túrós, G.I.; Éles, J.; Faigl, F.; Greiner, I., The route from problem to solution in multistep continuous flow synthesis of pharmaceutical compounds. *Bioorg. Med. Chem.* **2017**, *25*(23): 6180–6189.

15. Jolliffe, H.G.; Diab, S.; Gerogiorgis, D.I.; Nonlinear optimization via explicit NRTL model solubility prediction for antisolvent mixture selection in artemisinin crystallization. *Org. Process Res. Dev.* **2018**, *22*(1): 40–53.

16. Grom, M.; Stavber, G.; Drnovšek, P.; Likozar, B., Modelling chemical kinetics of a complex reaction network of active pharmaceutical ingredient (API) synthesis with process optimization for benzazepine heterocyclic compound. *Chem. Eng. J.* **2016**, *283*: 703–716.

17. Patel, M.P.; Shah, N.; Ashe, R., Robust optimisation methodology for the process synthesis of continuous technologies. *Comput. Aided Chem. Eng.* **2011**, *29*: 351–355.

18. Bédard, A.-C.; Adamo, A.; Aroh, K.C.; Russell, M.G.; Bedermann, A.A.; Torosian, J.; Yue, B.; Jensen, K.F.; Jamison, T.F., Reconfigurable system for automated optimization of diverse chemical reactions. *Science* **2018**, *361*(6408): 1220–1225.

19. Ott, D.; Kralisch, D.; Denčić, I.; Hessel, V.; Laribi, Y.; Perrichon, P.D.; Berguerand, C.; Kiwi-Minsker, L.; Loeb, P., Life cycle analysis within pharmaceutical process optimization and intensification: case study of active pharmaceutical ingredient production. *ChemSusChem* **2014**, *7*(12): 3521–3533.

20. Ott, D.; Borukhova, S.; Hessel, V., Life cycle assessment of multi-step rufinamide synthesis – from isolated reactions in batch to continuous microreactor networks. *Green Chem.* **2016**, *18*(4): 1096–1116.

21. Drageset, A.; Bjørsvik, H.-R., Continuous flow synthesis concatenated with continuous flow liquid–liquid extraction for work-up and purification: selective mono- and di-iodination of the imidazole backbone. *React. Chem. Eng.* **2016**, *1*(4): 436–444.

22. Monbaliu, J.-C.M.; Stelzer, T.; Revalor, E.; Weeranoppanant, N.; Jensen, K.F.; Myerson, A.S., Compact and integrated approach for advanced end-to-end production, purification, and aqueous formulation of lidocaine hydrochloride. *Org. Process Res. Dev.* **2016**, *20*(7): 1347–1353.

23. Weeranoppanant, N.; Adamo, A.; Saparbaiuly, G.; Rose, E.; Fleury, C.; Schenkel, B.; Jensen, K.F., Design of multistage counter-current liquid–liquid extraction for small-scale applications. *Ind. Eng. Chem. Res.* **2017**, *56*(14): 4095–4103.

24. Yang, Y.; Nagy, Z.K., Combined cooling and antisolvent crystallization in continuous mixed suspension, mixed product removal cascade crystallizers: steady-state and startup optimization. *Ind. Eng. Chem. Res.* **2015**, *54*(21): 5673–5682.

25. Ridder, B.J.; Majumder, A.; Nagy, Z.K., Population balance model-based multiobjective optimization of a multisegment multiaddition (MSMA) continuous plug-flow antisolvent crystallizer. *Ind. Eng. Chem. Res.* **2014**, *53*(11): 4387–4397.

26. Li, J.; Lai, T.C.; Trout, B.L.; Myerson, A.S., Continuous crystallization of cyclosporine: the effect of operating conditions on yield and purity. *Cryst. Growth Des.* **2017**, *17*(3): 1000–1007.

27. Acevedo, D.; Tandy, Y.; Nagy, Z.K., Multiobjective optimization of an unseeded batch cooling crystallizer for shape and size manipulation. *Ind. Eng. Chem. Res.* **2015**, *54*(7): 2156–2166.

28. Ridder, B.J.; Majumder, A.; Nagy, Z.K., Parametric, optimization-based study on the feasibility of

a multisegment antisolvent crystallizer for in situ fines removal and matching of target size distribution. *Ind. Eng. Chem. Res.* **2016**, *55*(8): 2371–2380.

29. Park, K.; Kim, D.Y.; Yang, D.R., Operating strategy for continuous multistage mixed suspension and mixed product removal (MSMPR) crystallization processes depending on crystallization kinetic parameters. *Ind. Eng. Chem. Res.* **2016**, *55*(6): 7142–7153.

30. Zhang, H.; Quon, J.; Alvarez, A.J.; Evans, J.; Myerson, A.S.; Trout, B., Development of continuous anti-solvent/cooling crystallization process using cascaded mixed suspension, mixed product removal crystallizers. *Org. Process Res. Dev.* **2012**, *16*(5): 915–924.

31. Lee, J.W.; Horváth, Z.; O'Brien, A.G.; Seeberger, P.H.; Seidel-Morgenstern, A., Design and optimization of coupling a continuously operated reactor with simulated moving bed chromatography. *Chem. Eng. J.* **2014**, *251*: 355–370.

32. Denčić, I.; Ott, D.; Kralisch, D.; Noel, T.; Meuldijk, J.; de Croon, M.; Hessel, V.; Laribi, Y.; Perrichon, P., Eco-efficiency analysis for intensified production of an active pharmaceutical ingredient: a case study. *Org. Process Res. Dev.* **2014**, *18*(11): 1326–1338.

33. Correia, C.A.; Gilmore, K.; McQuade, D.T.; Seeberger, P.H., A concise flow synthesis of efavirenz. *Angew. Chemie Int. Ed.* **2015**, *54*(16): 4945–4948.

34. Kuehn, S.E., 2015, Janssen embraces continuous manufacturing for Prezista, *Pharmaceutical Manufacturing*. Available at: http://www.pharmamanufacturing.com/articles/2015/janssen-embraces-continuous-manufacturing-for-prezista/.

35. PharmaTech, 2016, FDA approves tablet production on janssen continuous manufacturing line.

36. Mandala, D.; Chada, S.; Watts, P., Semi-continuous multi-step synthesis of lamivudine. *Org. Biomol. Chem.* **2017**, *15*(16): 3444–3454.

37. Ziegler, R.E.; Desai, B.K.; Jee, J.-A.; Gupton, B.F.; Roper, T.D.; Jamison, T.F., 7-step flow synthesis of the hiv integrase inhibitor dolutegravir. *Angew. Chemie* **2018**, *57*:1–6.

38. Kuminek, G.; Rodríguez-Hornedo, N.; Siedler, S.; Rocha, H.V.A.; Cuffini, S.L.; Cardoso, S.G., How cocrystals of weakly basic drugs and acidic coformers might modulate solubility and stability. *Chem. Commun.* **2016**, *52*(34): 5832–5835.

39. Hargrave, K.D.; Proudfoot, J.R.; Grozinger, K.G.; Cullen, E.; Kapadia, S.R.; Patel, U.R.; Fuchs, V.U.; Mauldin, S.C.; Vitous, J.; Behnke, M.L.; Klunder, J.M.; Pal, K.; Skiles, J.W.; McNeil, D.W.; Rose, J.M.; Chow, G.C.; Skoog, M.T.; Wu, J.C.; Schmidt, G.; Engel, W.W.; Eberlein, W.G.; Saboe, T.D.; Campbell, S.J.; Rosenthal, A.S.; Adams, J., Novel non-nucleoside inhibitors of HIV-1 reverse transcriptase. 1. Tricyclic pyridobenzo- and dipyridodiazepinones. *J. Med. Chem.* **1991**, *34*(7): 2231–2241.

40. Macha, S.; Yong, C.L.; Darrington, T.; Davis, M.S.; MacGregor, T.R.; Castles, M.; Krill, S.L., In vitro-in vivo correlation or nevirapine extended release tablets. *Biopharm. Drug Dispos.* **2009**, *30*(9): 542–550.

41. Cheeseman, S.H.; Hattox, S.E.; McLaughlin, M.M.; Koup, R.A.; Andrews, C.; Bova, C.A.; Pav, J.W.; Roy, T.; Sullivan, J.L.; Keirns, J.J., Pharmacokinetics of nevirapine: initial single-rising-dose study in humans. *Antimicrob. Agents Chemother.* **1993**, *37*(2): 178–82.

42. Sheldon, R.A., Fundamentals of green chemistry: efficiency in reaction design. *Chem. Soc. Rev.* **2012**, *41*(4): 1437–1451.

43. Roschangar, F.; Sheldon, R.A.; Senanayake, C.H., Overcoming barriers to green chemistry in the pharmaceutical industry – the Green Aspiration Level™ concept. *Green Chem.* **2015**, *17*(2): 752–768.

44. Couper, J.R., 2003, *Process Engineering Economics*, CRC Press.

45. Woods, D.R., 2007, *Rules of Thumb in Engineering Practice*, Wiley.

46. Diab, S.; Gerogiorgis, D.I., Process modeling, simulation, and technoeconomic evaluation of separation solvents for the continuous pharmaceutical manufacturing (CPM) of diphenhydramine. *Org. Process Res. Dev.* **2017**, *21*(7): 924–946.

47. Jolliffe, H.G.; Gerogiorgis, D.I., Technoeconomic optimisation and comparative environmental impact evaluation of continuous crystallisation and antisolvent selection for artemisinin recovery, *Comput. Chem. Eng.* **2017**, *103*: 218–232.

48. Diab, S.; Gerogiorgis, D.I., Process modelling, simulation and technoeconomic evaluation of crystallisation antisolvents for the continuous pharmaceutical manufacturing of rufinamide. *Comput. Chem. Eng.* **2018**, *111*: 102–114.

49. Papavasileiou, V.; Koulouris, A.; Siletti, C.; Petrides, D., Optimize manufacturing of pharmaceutical products with process simulation and production scheduling tools. *Chem. Eng. Res. Des.* **2007**, *85*(7): 1086–1097.

50. Wu, H.; Dong, Z.; Li, H.; Khan, M., An integrated process analytical technology (PAT) approach for pharmaceutical crystallization process understanding to ensure product quality and safety: FDA scientist's perspective. *Org. Process Res. Dev.* **2015**, *19*: 89–101.

51. Henderson, R.K.; Jiménez-González, C.; Constable, D.J.C.; Alston, S.R.; Inglis, G.G.A.; Fisher, G.; Sherwood, J.; Binks, S.P.; Curzons, A.D., Expanding GSK's solvent selection guide – embedding sustainability into solvent selection starting at medicinal chemistry. *Green Chem.* **2011**, *13*(4): 854–862.

52. Jolliffe, H.G.; Gerogiorgis, D.I., Process modelling, design and technoeconomic evaluation for continuous paracetamol crystallisation. *Comput. Chem. Eng.* **2018**, *118*, 224–235.

53. Hill., A.; Barber, M.; Gotham, D., Estimated costs of production and potential prices for the WHO Essential Medicines List. *BMJ Brit. Med. J.* **2018**, *3*: 1–7.

54. Jolliffe, H.G.; Gerogiorgis, D.I., Technoeconomic optimization of a conceptual flowsheet for continuous separation of an analgaesic Active Pharmaceutical Ingredient (API). *Ind. Eng. Chem. Res.* **2017**, *56*(15), 4357–4376.

1
2
3
4
5
6
7
8
9
10
11
12
13
14
15
16
17
18
19
20
21
22
23
24
25
26
27
28
29
30
31
32
33
34
35
36
37
38
39
40
41
42
43
44
45
46
47
48
49
50
51
52
53
54
55
56
57
58
59
60

GRAPHICAL ABSTRACT

183x115mm (300 x 300 DPI)